

# Thermomagnetic Phenomena in Antimony in the Phonon Drag Region

M. S. Bresler and N. A. Red'ko

*Institute of Semiconductors, USSR Academy of Sciences*

Submitted December 21, 1971

Zh. Eksp. Teor. Fiz. 62, 1867-1883 (May, 1972)

The temperature variation (2-100°K) of the thermal-e.m.f.  $\alpha_{ij}$  and Nernst coefficient  $Q_{ij} = \alpha_{ij}(H)/H$  of single crystal antimony samples oriented along the principal crystallographic directions ( $C_1, C_2, C_3$ ) is investigated. A comparison with the theory reveals that phonon drag of the current carries at low temperatures should play a large role. The Umkehr-effekt is observed for the thermo-e.m.f. tensor components and the experimental data are in good agreement with the calculations taking into account the phonon drag and also the inequality of the electron and hole concentrations ( $\Delta N = (p - n)$  (at  $T \approx 4^\circ K$ )).

**I**NVESTIGATIONS of thermomagnetic phenomena in semiconductors and in metals yield information both on the structure of the energy spectrum of the carrier and on the carrier interaction with phonons and impurities that cause scattering.

In spite of the large number of investigations of various properties of antimony (the carrier energy spectrum was investigated in detail by various methods<sup>[1]</sup>), the investigations of the thermomagnetic phenomena in antimony below room temperature were not systematic until recently. Thus, Saunders and Oktu<sup>[2]</sup> investigated the thermoelectric power of antimony (without a magnetic field) only down to liquid-nitrogen temperature, and have shown that the experimental results can be interpreted on the basis of a multivalley model of the carrier energy spectrum, with allowance for only the diffusion contribution to the thermoelectric power. Grenier and co-workers<sup>[3,4]</sup> cite data that point to an appreciable role of phonon dragging at low temperatures, but the results are limited to helium temperatures and are interpreted within the framework of a rather crude isotropic model. One of the authors and Shalyt<sup>[5]</sup> reported preliminary results of the measurement of the Nernst coefficient of a pure antimony specimen in a wide temperature interval, down to 2°K, and have shown that the phonon dragging effect predominates below nitrogen temperatures.

We develop in this paper a theory of thermomagnetic phenomena in antimony, with allowance for the multivalley structure of the carrier energy spectrum, and report and discuss experimental results on the thermoelectric power of antimony in magnetic fields at temperatures below 20°K, when the contribution of the phonon dragging to the thermomagnetic coefficients exceeds the diffusion contribution.

## 1. THEORY OF THERMOELECTRIC POWER OF ANTIMONY IN A MAGNETIC FIELD

The kinetic coefficients are defined as the proportionality coefficients in the expansion of the thermodynamic fluxes (the electric current  $j$  and the heat flow  $w$ ) in terms of generalized forces (the electric field  $E$  and the temperature gradient  $\nabla T$ ):

$$j = \hat{\sigma}E - \hat{\beta}\nabla T, \quad w = \hat{\delta}E - \hat{\gamma}\nabla T. \quad (1)$$

The quantities calculated in the theory are the electric conductivity tensor  $\hat{\sigma}$  and the thermoelectric tensor  $\hat{\beta}$ , and the measured quantities are the resistivity tensor  $\hat{\rho} = \hat{\sigma}^{-1}$  and the thermoelectric-power tensor

$$\hat{\alpha} = \hat{\sigma}^{-1}\hat{\beta} = \hat{\rho}\hat{\beta}, \text{ and also the thermal conductivity tensor } \hat{\kappa} = \hat{\gamma} - \hat{\delta}\hat{\sigma}^{-1}\hat{\beta} \text{ (according to the Onsager relation, } \delta_{ik}(H) = \beta_{ki}(H)T).$$

In the evaluation of the experimental results, it is also necessary to recognize that the thermomagnetic effects are usually measured under adiabatic conditions (i.e., in the absence of a heat flow perpendicular to the sample length), whereas in the theory it is convenient to use isothermal quantities corresponding to the absence of a transverse temperature gradient. The influence of the non-isothermy will be considered in the second section.

By investigating the symmetry properties of the antimony crystal (point group  $D_{3d}$ ), it is easy to determine the number of independent components (and to establish relations between the mutually dependent components) both for the case when there is no magnetic field and in the case when the magnetic field is oriented along the most symmetrical directions in the crystal ( $H \parallel C_2, H \parallel C_1, H \parallel C_3$ ). We shall consider only these symmetrical cases, since the analysis of the experimental results is difficult when the magnetic field direction is arbitrary.

To find the thermoelectric-power tensor  $\hat{\alpha}$  it is necessary to calculate the tensors  $\hat{\sigma}$  and  $\hat{\beta}$ .

The electric conductivity  $\hat{\sigma}$  (in a magnetic field) was calculated by us earlier<sup>[6]</sup>. We present here only expressions for the thermoelectric tensor  $\hat{\beta}$ , calculated under the same assumptions as in<sup>[6]</sup>, i.e., for a multivalley carrier spectrum consisting of six hole and three electron ellipsoids lying in mirror-symmetry planes and inclined at angles  $\varphi_h$  and  $\varphi_e$  to the basal plane.

It is assumed that it is possible to introduce a relaxation-time tensor that is diagonal in terms of the mass ellipsoid; in addition, the electron and hole densities are assumed equal,  $n = p = N$  (unless otherwise stipulated).

In accordance with the standard notation, we choose the 1 axis to be the binary axis  $C_2$  of the crystal, the 2 axis is the bisector direction  $C_1$ , and the 3 axis is the trigonal axis  $C_3$ .

When thermoelectric phenomena at low temperatures are considered, it is important to take into account the deviation of the phonon distribution from equilibrium (i.e., the dragging of the carriers by the phonons). We have therefore calculated the contribution made to the tensor  $\hat{\beta}$  both by the dragging effect and by the direct action of the temperature gradient on the carrier system (the "diffusion" contribution). We consider in this section only the calculation of the phonon contribution to  $\hat{\beta}$ , and the results for the diffusion part of the tensor  $\hat{\beta}$

are given in the Appendix (they were used by us only to estimate the role of the diffusion part in comparison with the phonon part, and are presented only because, in so far as we know, there are no published calculations of the diffusion part of the tensor  $\hat{\beta}$  with allowance for the structure of the energy spectrum of the carriers in antimony).

The influence of the dragging of the carriers by the phonons on the thermomagnetic phenomena in semimetals was considered in [7-9], where it was shown that in the case of sufficiently strong dragging ( $L_e < L_f$ , where  $L_e$  and  $L_f$  are the phonon mean free paths for scattering by electrons and phonons, respectively), the phonon contribution to the thermoelectric power does not contain the small parameter  $kT/\xi$  ( $\xi$  is the Fermi energy), i.e., it exceeds greatly the diffusion contribution. In the indicated papers, however, the carrier energy spectrum is assumed to be isotropic; the anisotropy for the real energy spectrum of bismuth was accounted for by Korenblit [10].

Korenblit [10] has shown that the thermoelectric-power tensor can be represented in the presence of the dragging effect as a sum of contributions made by different groups of carriers  $s$ , corresponding to different valleys of the multivalley model:

$$\alpha_{ni}(\mathbf{H}) = \rho_{nm}(\mathbf{H}) \sum_s \sigma_{mk}^{(s)}(\mathbf{H}) a_{ki}^{(s)} = \rho_{nm}(\mathbf{H}) \beta_{mi}(\mathbf{H}). \quad (2)$$

where  $\sigma_{mk}^{(s)}$  is the partial electric conductivity of the given group of carriers (summation over repeated indices is implied).

The tensor of the partial thermoelectric power of the specified group of carriers can be represented in the form

$$\alpha_{ki}^{(s)} = \sum_{\mu} a_{ki}^{(\mu,s)} = \frac{1}{n^{(s)} e^{(s)} (kT)^2} \sum_{\mu} \int \frac{d^3q}{(2\pi\hbar)^3} \times \frac{\exp(\hbar\omega_q^{(s)}/kT) \hbar\omega_q^{(s)} \nu^{(\mu,s)}(q)}{[\exp(\hbar\omega_q^{(s)}/kT) - 1]^2} S_l^{(\mu)} q_k^{(s)}, \quad (3)$$

where  $n^{(s)}$  and  $e^{(s)}$  are the concentration and charge of the carriers of group  $s$ ,  $\mu$  is the number of the acoustic branch of the phonons,  $S_l^{(\mu)}$  is the  $l$ -component of the group velocity of the phonons of group  $\mu$ ,  $\nu^{(\mu,s)}$  is the relaxation frequency of the phonons of branch  $\mu$  on the carriers of group  $s$ , and  $\nu^{(\mu)}$  is the total relaxation frequency of the phonons of branch  $\mu$  on the carriers of all groups of phonons and defects.

The integration is over a space-space volume  $\Omega_S$  that includes the wave vectors of the phonons interacting with the carriers of the given group  $s$  (this volume is an ellipsoid whose semiaxes are double the semiaxis of the constant energy surface  $\epsilon_S(\mathbf{p}) = \xi$ ), with  $\nu^{(\mu,s)} \neq 0$  inside this volume and  $\nu^{(\mu,s)} = 0$  outside it.

Since the phonon-phonon collision frequency decreases rapidly with decreasing temperature, it follows that at low temperatures, starting with a certain temperature  $T_f$  (corresponding to the condition  $\nu^{(\mu)} \approx \nu^{(\mu,s)}$ ), the scattering of phonons by electrons begins to prevail over all other phonon-scattering mechanisms. We can also introduce another characteristic temperature  $T_0 \sim \sqrt{2m^* \xi S^2/k}$ , which determines the upper limit of the region in which all the excited phonons can interact with the carriers.

If  $T_0 < T_f$ , then in the temperature region  $T_0 < T$

$< T_f$  all the phonons whose interaction with the carriers is allowed by the conservation laws are scattered by carriers, and the partial thermoelectric power depends on neither the temperature nor the magnetic field and reaches a maximum possible value on the order of  $k/e$  ( $4k/3e$  for an isotropic spectrum).

If  $T < T_0$ , the phonons that drag the carriers start to freeze out, and the partial thermoelectric power decreases rapidly with temperature,  $\alpha \sim T^3$ .

If  $T_f < T_0$ , there is no region where the partial thermoelectric power is independent of the temperature, and all we have is a maximum of the partial thermoelectric power near a temperature close to  $T_f$ , but this maximum does not reach the largest value  $\sim k/e$ , but has a much lower value determined by the ratio  $\nu^{(\mu,s)}/\nu^{(\mu)}$ . At  $T \ll T_f$  there is likewise a temperature dependence of the  $T^3$  type.

It is obvious that in the case of a multivalley ellipsoidal spectrum it is necessary to introduce a set of values  $T_f$  and  $T_0$  corresponding to different carrier groups.

The influence of the anisotropy will be considered in greater detail in the discussion of the experimental data.

Korenblit [10] calculated the partial thermoelectric power of the electrons and holes for bismuth at  $T > T_0$  (and  $T_0 < T_f$ ), under the assumption that the elongated shape of the electron-mass ellipsoids causes the region of intersection of the volumes  $\Omega_S$  corresponding to different ellipsoids to be small, i.e., the phonons interacting with one carrier group  $s$  hardly interact with all the other groups  $s'$ . In addition, the true phonon spectrum of bismuth was replaced by the spectrum of a transversely-isotropic medium.

The results of these calculations agree satisfactorily with the experimental data on the thermoelectric power of bismuth [11].

For antimony, however, it is impossible to realize such a program since, first, it is impossible to simplify suitably the phonon spectrum, and second, the assumption concerning the intersections with the phase volumes should be satisfied much worse for antimony than for bismuth for phonons interacting with carriers in different ellipsoids, since the mass-ellipsoid anisotropy for the electrons and holes is smaller. To calculate the thermoelectric power tensor in a magnetic field in the presence of the dragging effect, we have therefore introduced phenomenologically the tensors of the electron and hole partial thermoelectric powers, and obtained the final result for the tensor  $\hat{\beta}$  by summing the contributions of different carrier groups:

$$\beta_{mi} = \sum_s \sigma_{mk}^{(s)} a_{ki}^{(s)}. \quad (4)$$

Since the electron ellipsoids in bismuth and of the electron and hole mass ellipsoids in antimony have the same symmetry, it is natural to specify, in the phenomenological approach, the tensor of the partial thermoelectric power for one ellipsoid (in terms of the crystal axes) in the form

$$\begin{pmatrix} \alpha_1 & 0 & 0 \\ 0 & \alpha_2 & \alpha_4 \\ 0 & \alpha_5 & \alpha_3 \end{pmatrix} \quad (5)$$

(the partial thermoelectric power tensors are obtained for the two other ellipsoids by rotating the coordinate axes through  $\pm 120^\circ$ ). This form of the partial thermo-

electric power for electrons in bismuth is obtained with allowance for the anisotropy of the phonon spectrum at a sufficiently large anisotropy,  $\alpha_4 \neq \alpha_5$  (i.e., the partial thermoelectric power is asymmetrical relative to the ellipsoid axes).

Summing the contributions from the individual ellipsoids in accord with (4), we can obtain the thermoelectric tensor  $\hat{\beta}$  with allowance for the dragging effect, expressed in terms of the tensors of the mobility tensors  $\mu_{j-}$  of the electrons and  $\mu_{j+}$  of the holes and the partial thermoelectric powers  $\alpha_{j\pm}$ .

Since the general expression for the tensor  $\hat{\beta}$  is very cumbersome even if the magnetic field  $\mathbf{H}$  is oriented in a symmetrical direction, we present the expression for the tensor  $\hat{\beta}$  only for a strong magnetic field and will not write out in explicit form the expressions for the thermoelectric power tensor  $\hat{\alpha}$ ; we shall be interested only in the asymptotic behavior of the components of the thermoelectric power tensor in a magnetic field.

The results for the tensor  $\hat{\beta}$ , with allowance for the dragging effect, take the following form in the case  $\mathbf{H} \parallel \mathbf{C}_2 \parallel 1$

$$\beta_{11} = 3 \sum \left[ \frac{\mu_{3i}^2 \mu_{3i} \alpha_{4i} + \mu_{3i} \mu_{2i} \mu_{3i} \alpha_{4i} - \mu_{3i} \mu_{4i}^2 \alpha_{4i}}{\mu_{3i} (3\mu_{1i} + \mu_{2i}) - \mu_{4i}^2} + \frac{2\mu_{1i} \mu_{2i} \mu_{3i} \alpha_{2i} - 2\mu_{1i} \mu_{4i}^2 \alpha_{2i}}{\mu_{3i} (3\mu_{1i} + \mu_{2i}) - \mu_{4i}^2} \right], \quad (6)$$

$$\beta_{22} = -3 \sum Z_i \frac{\mu_{1i} \mu_{4i} (\alpha_{1i} - \alpha_{2i})}{\mu_{3i} (3\mu_{1i} + \mu_{2i}) - \mu_{4i}^2} \left( \frac{H}{c} \right)^{-1}, \quad (7)$$

$$\beta_{23} = -3 \sum Z_i \left[ \frac{2\mu_{1i} \mu_{4i}}{\mu_{3i} (3\mu_{1i} + \mu_{2i}) - \mu_{4i}^2} \alpha_{4i} - \alpha_{3i} \right] \left( \frac{H}{c} \right)^{-1}, \quad (8)$$

$$\beta_{32} = -\frac{3}{2} \sum Z_i \left[ \frac{\mu_{3i} (\mu_{1i} - \mu_{2i}) + \mu_{4i}^2}{\mu_{3i} (3\mu_{1i} + \mu_{2i}) - \mu_{4i}^2} (\alpha_{1i} - \alpha_{2i}) + \alpha_{1i} + \alpha_{2i} \right] \left( \frac{H}{c} \right)^{-1}, \quad (9)$$

$$\beta_{33} = -3 \sum Z_i \frac{\mu_{3i} (\mu_{1i} - \mu_{2i}) + \mu_{4i}^2}{\mu_{3i} (3\mu_{1i} + \mu_{2i}) - \mu_{4i}^2} \alpha_{4i} \left( \frac{H}{c} \right)^{-1}. \quad (10)$$

Here and below, the symbols  $\Sigma$  denote summation with respect to  $i$  over the hole (+) and electron (-) carrier groups;  $Z_+ = 1$ ,  $Z_- = -1$ ,  $\mu_{1i}$ ,  $\mu_{2i}$ ,  $\mu_{3i}$ , and  $\mu_{4i}$  are the components of the mobility tensor relative to the crystal axes;  $\alpha_{1i}$ ,  $\alpha_{2i}$ ,  $\alpha_{3i}$ , and  $\alpha_{4i}$  are the components of the partial thermoelectric power tensor.

In strong magnetic field, such that

$$\mathcal{H}_+, \mathcal{H}_-, \mathcal{E}_+, \mathcal{E}' > (H/c)^{-2}, \quad (11)$$

where

$$\mathcal{H}_i = \mu_{2i} \mu_{3i} - \mu_{4i}^2, \quad \mathcal{E}_i = 1/4 (3\mu_{1i} \mu_{3i} + \mu_{2i} \mu_{3i} - \mu_{4i}^2),$$

the asymptotic behavior of the components of the thermoelectric power tensor is given by

$$\alpha_{11} \sim H^0, \quad \alpha_{22} \sim H, \quad \alpha_{23} \sim H, \quad \alpha_{32} \sim H, \quad \alpha_{33} \sim H. \quad (12)$$

The presence of a contribution linear in  $H$  to the diagonal part of the thermoelectric power tensor is the well known Umkehr effect, which is connected with the inclinations of the electron and hole mass ellipsoids to the crystal axes, and which becomes particularly strongly manifest in strong magnetic fields for semimetals ( $n = p$ ).

If there is a weak unbalance between the hole and electron densities,  $\Delta N = p - n \neq 0$ , then the asymptotic forms of the components of the tensor  $\hat{\rho}$  changes in the magnetic field region defined by the inequalities

$$\frac{\Delta N}{N} \frac{H}{c} \left[ \frac{\mu_{4+}}{3} \left( \frac{1}{\mathcal{H}_+} - \frac{1}{\mathcal{E}_+} \right) + \frac{\mu_{4-}}{3} \left( \frac{1}{\mathcal{H}_-} - \frac{1}{\mathcal{E}_-} \right) \right]^{-1} > 1, \quad (13)$$

and

$$\frac{\Delta N}{N} \frac{H}{c} 3 \left[ \left( \frac{\mu_{3+}}{I_+} + \frac{2\mu_{3+}}{\mathcal{H}_+} + \frac{\mu_{3-}}{I_-} + \frac{2\mu_{3-}}{\mathcal{H}_-} \right) \left( \frac{\mu_{2+}}{\mathcal{E}_+} + \frac{\mathcal{E}_+}{\mathcal{H}_+} + \frac{\mu_{2-}}{\mathcal{E}_-} + \frac{\mathcal{E}_-}{\mathcal{H}_-} \right) \right]^{-1/2} < 1, \quad (14)$$

$$I_i = 1/2 (\mu_{1i} + 3\mu_{2i}), \quad \mathcal{E}_i = 1/2 (3\mu_{1i} + \mu_{2i}),$$

and we obtain for the tensor  $\hat{\alpha}$ :

$$\alpha_{11} \sim H^0, \quad \alpha_{22} \sim H^2, \quad \alpha_{23} \sim H^2, \quad \alpha_{32} \sim H^2, \quad \alpha_{33} \sim H^2. \quad (15)$$

We shall henceforth call this magnetic-field region "intermediate."

If an equality inverse to (14) is satisfied, then

$$\alpha_{11} \sim H^0, \quad \alpha_{22} \sim H^0, \quad \alpha_{23} \sim H^0, \quad \alpha_{32} \sim H^0, \quad \alpha_{33} \sim H^0 \quad (16)$$

(henceforth called the region of "extremely strong" fields).

In the case  $\mathbf{H} \parallel \mathbf{C}_1 \parallel 2$  we have

$$\beta_{11} = \sum \left[ \frac{\alpha_{4i}}{\mu_{3i}} + 2 \frac{\mu_{1i} \alpha_{4i} + 3\mu_{2i} \alpha_{2i} + 3\mu_{4i} \alpha_{3i}}{(\mu_{1i} + 3\mu_{2i}) \mu_{3i} - 3\mu_{4i}^2} \right] \left( \frac{H}{c} \right)^{-2},$$

$$\beta_{12} = -\sum Z_i \left[ \frac{\mu_{4i}}{\mu_{3i}} \alpha_{2i} - \frac{(3\alpha_{1i} + \alpha_{2i}) \mu_{1i} \mu_{4i}}{(\mu_{1i} + 3\mu_{2i}) \mu_{3i} - 3\mu_{4i}^2} \right] \left( \frac{H}{c} \right)^{-1},$$

$$\beta_{13} = -\sum Z_i \left[ \alpha_{3i} + \frac{\mu_{4i}}{\mu_{3i}} \alpha_{4i} + \frac{2\mu_{1i} \mu_{4i} \alpha_{4i}}{(\mu_{1i} + 3\mu_{2i}) \mu_{3i} - 3\mu_{4i}^2} \right] \left( \frac{H}{c} \right)^{-1},$$

$$\beta_{21} = \sum Z_i \left[ \frac{\mu_{4i}}{\mu_{3i}} \alpha_{4i} - \frac{(\alpha_{1i} + 3\alpha_{2i}) \mu_{1i} \mu_{4i}}{(\mu_{1i} + 3\mu_{2i}) \mu_{3i} - 3\mu_{4i}^2} - \frac{3\alpha_{3i} (\mu_{1i} \mu_{3i} - \mu_{2i} \mu_{3i} + \mu_{4i}^2)}{(\mu_{1i} + 3\mu_{2i}) \mu_{3i} - 3\mu_{4i}^2} \right] \left( \frac{H}{c} \right)^{-1},$$

$$\beta_{22} = \sum \left[ \left( \mu_{2i} - \frac{\mu_{4i}^2}{\mu_{3i}} \right) \alpha_{2i} + \frac{1}{2} (3\alpha_{1i} + \alpha_{2i}) \frac{\mu_{1i} (\mu_{2i} \mu_{3i} - \mu_{4i}^2)}{(\mu_{1i} + 3\mu_{2i}) \mu_{3i} - 3\mu_{4i}^2} \right],$$

$$\beta_{23} = \sum \left[ \left( \mu_{2i} - \frac{\mu_{4i}^2}{\mu_{3i}} \right) \alpha_{4i} - \frac{\mu_{1i} (\mu_{2i} \mu_{3i} - \mu_{4i}^2)}{(\mu_{1i} + 3\mu_{2i}) \mu_{3i} - 3\mu_{4i}^2} \alpha_{4i} \right], \quad (17)$$

$$\beta_{31} = \frac{3}{2} \sum Z_i \left[ \alpha_{1i} + \alpha_{2i} + (\alpha_{1i} - \alpha_{2i}) \right.$$

$$\left. \times \frac{\mu_{1i} \mu_{3i} - \mu_{2i} \mu_{3i} + \mu_{4i}^2}{(\mu_{1i} + 3\mu_{2i}) \mu_{3i} - 3\mu_{4i}^2} \right] \left( \frac{H}{c} \right)^{-1},$$

$$\beta_{32} = \sum \left[ \frac{\mu_{4i}}{\mu_{1i} \mu_{3i}} \alpha_{2i} + \frac{\alpha_{3i}}{\mu_{1i}} - \frac{4\mu_{1i} \alpha_{2i} + \mu_{3i} \alpha_{3i}}{(\mu_{1i} + 3\mu_{2i}) \mu_{3i} - 3\mu_{4i}^2} \right] \left( \frac{H}{c} \right)^{-2}$$

$$\beta_{33} = \sum \left[ \frac{\mu_{4i}}{\mu_{1i} \mu_{3i}} \alpha_{4i} + \frac{\alpha_{3i}}{\mu_{1i}} + \frac{8\mu_{1i} \alpha_{4i} + 2\mu_{3i} \alpha_{3i}}{(\mu_{1i} + 3\mu_{2i}) \mu_{3i} - 3\mu_{4i}^2} \right] \left( \frac{H}{c} \right)^{-2}.$$

The asymptotic behavior of  $\hat{\alpha}$  in strong field is given

$$\mu_{1i} \mu_{3i} \left( \frac{H}{c} \right)^2, \quad \frac{1}{4} (\mu_{1i} \mu_{3i} + 3\mu_{2i} \mu_{3i} - 3\mu_{4i}^2) \left( \frac{H}{c} \right)^2 > 1, \quad (18)$$

$$\alpha_{11} \sim H^0, \quad \alpha_{12} \sim H, \quad \alpha_{13} \sim H, \quad \alpha_{21} \sim H^{-1}, \quad \alpha_{22} \sim H^0,$$

$$\alpha_{23} \sim H^0, \quad \alpha_{31} \sim H, \quad \alpha_{32} \sim H^0, \quad \alpha_{33} \sim H^0. \quad (19)$$

In "intermediate" fields we have

$$\alpha_{11} \sim H^2, \quad \alpha_{12} \sim H, \quad \alpha_{13} \sim H, \quad \alpha_{21} \sim H, \quad \alpha_{22} \sim H^2, \quad (20)$$

$$\alpha_{23} \sim H^2, \quad \alpha_{31} \sim H, \quad \alpha_{32} \sim H^2, \quad \alpha_{33} \sim H^2.$$

In extremely strong fields we have

$$\alpha_{11} \sim H^0, \quad \alpha_{12} \sim H^{-1}, \quad \alpha_{13} \sim H^{-1}, \quad \alpha_{21} \sim H^{-1}, \quad \alpha_{22} \sim H^0, \quad (21)$$

$$\alpha_{23} \sim H^0, \quad \alpha_{31} \sim H^{-1}, \quad \alpha_{32} \sim H^0, \quad \alpha_{33} \sim H^0.$$

The exact criteria delineating the region of "intermediate" and extremely strong fields are given in this case by very cumbersome formulas. They can be readily obtained from the results of [6].

In the case  $\mathbf{H} \parallel \mathbf{C}_3 \parallel 3$  we have

$$\begin{aligned}\beta_{11} &= \frac{3}{2} \sum \frac{\mu_{1i}\alpha_{1i} + \mu_{2i}\alpha_{2i} + \mu_{3i}\alpha_{3i}}{\mu_{1i}\mu_{2i}}, \\ \beta_{12} = -\beta_{21} &= \frac{3}{2} \sum Z_i \left( \alpha_{1i} + \alpha_{2i} + \frac{\mu_{1i}}{\mu_{2i}} \alpha_{3i} \right) \left( \frac{H}{c} \right)^{-1}, \\ \beta_{33} &= 3 \sum \frac{\mu_{2i}\mu_{3i} - \mu_{1i}^2}{\mu_{2i}} \alpha_{3i}.\end{aligned}\quad (22)$$

In strong magnetic fields

$$\mu_{1+}\mu_{2+}(H/c)^2, \quad \mu_{1-}\mu_{2-}(H/c)^2 > 1, \quad (23)$$

$$\alpha_{11} \sim H^0, \quad \alpha_{12} \sim H, \quad \alpha_{33} \sim H^0. \quad (24)$$

In "intermediate" fields

$$\frac{\Delta N}{N} \left( \frac{H}{c} \right)^2 \left( \frac{1}{\mu_{1-}\mu_{2-}} - \frac{1}{\mu_{1+}\mu_{2+}} \right)^{-1} > 1, \quad (25)$$

$$\begin{aligned}\frac{\Delta N}{N} \frac{2\mu_{2+}\mu_{3-}}{\mu_{2+} + \mu_{2-}} \frac{H}{c} < 1, \\ \alpha_{11} \sim H^2, \quad \alpha_{12} \sim H, \quad \alpha_{33} \sim H^0.\end{aligned}\quad (26)$$

In extremely strong fields (the inequality inverse to (26) is satisfied):

$$\alpha_{11} \sim H^0, \quad \alpha_{12} \sim H^{-1}, \quad \alpha_{33} \sim H^0. \quad (27)$$

## 2. EXPERIMENTAL RESULTS AND DISCUSSION

The thermomagnetic effects were measured on the single-crystal antimony specimens used in<sup>[6]</sup>, Sb I ( $\nabla T \parallel \mathbf{C}_1$ ), Sb II ( $\nabla T \parallel \mathbf{C}_2$ ), and Sb III ( $\nabla T \parallel \mathbf{C}_3$ ), oriented along the principal crystallographic axes: bisector  $\mathbf{C}_1$ , binary  $\mathbf{C}_2$ , and trigonal  $\mathbf{C}_3$  ( $\nabla T$  is the temperature gradient along the sample), with dimensions: Sb I— $50 \times 3.8 \times 2.8 \text{ mm}^3$ , Sb II— $50 \times 3 \times 2.4 \text{ mm}^3$  and Sb III— $28 \times 2.5 \times 2.1 \text{ mm}^3$ . We shall therefore use the hole and electron mobility data obtained in<sup>[6]</sup> in all the estimates and calculations that follow.

The investigated specimen was fused into the bottom of a vacuum chamber ( $\approx 18 \text{ mm}$  dia) which was immersed in the thermostating liquid (helium, hydrogen, nitrogen). The end of the specimen was in direct contact with the liquid helium, and this enabled us to investigate the thermoelectric and thermomagnetic effects down to temperatures  $\sim 2^\circ \text{K}$  on antimony specimens of relatively large cross section.

To investigate the temperature dependence of the kinetic coefficients of antimony above the temperature of liquid helium, the thermal contact between the specimen and the thermostating liquid was made worse by using a metal cap to seal the bottom of the chamber, through which the end of the specimen passed.

The temperature was measured at two points of the specimen and at constant heat flow in the following manner: with carbon resistors in the range  $T = 2-40^\circ \text{K}$  and with copper-constantan thermocouples in the range  $T = 30-300^\circ \text{K}$ . The thermoelectric power of the specimens was measured paired with copper, the absolute thermoelectric power of which was found not to exceed  $1 \mu \text{V/deg}$  in the entire temperature range.

The thermomagnetic effects in antimony were measured in a stationary magnetic field of intensity up to  $30 \text{ kOe}$ , which was oriented along one of the principal crystallographic directions ( $\mathbf{H} \parallel \mathbf{C}_2$ ,  $\mathbf{H} \parallel \mathbf{C}_1$ ,  $\mathbf{H} \parallel \mathbf{C}_3$ ). In the case  $\mathbf{H} \parallel \mathbf{C}_1$  we did not measure all the components

of the tensor  $\hat{\alpha}$ , and the theoretical analysis of the results is furthermore made difficult in this case by the very cumbersome calculations. We shall therefore discuss primarily the results for the two more symmetrical field orientations,  $\mathbf{H} \parallel \mathbf{C}_3$  and  $\mathbf{H} \parallel \mathbf{C}_2$ .

The sign of the voltage picked off the transverse probes was always reversed when the magnetic field was reversed, i.e., the contribution to the off-diagonal components of the tensor  $\hat{\alpha}$  were always odd in the field. The experimental results will therefore henceforth be represented not by the off-diagonal component of  $\hat{\alpha}$ , but by the Nernst coefficient, defined by

$$\alpha_{21} = \frac{E_2}{\nabla_1 T} = -Q_{21}^{(s)} H_3 \text{ or } \alpha_{32} = \frac{E_3}{\nabla_2 T} = -Q_{32}^{(s)} H_1.$$

Since the thermomagnetic effects were measured under adiabatic rather than isothermal conditions, it was necessary to estimate the influence of the produced transverse temperature gradient on the measurement results. The correction to the main effect (for example from  $\alpha_{12}$  to  $\alpha_{11}$  at  $\mathbf{H} \parallel \mathbf{C}_3$ ) necessitated by the non-isothermy is proportional to the ratio  $\kappa_{21}/\kappa_{22}$ , where  $\kappa_{21}$  describes the Righi-Leduc effect. In strong fields,  $\alpha_{11} \sim H$  and the correction term  $\alpha_{12}\kappa_{21}/\kappa_{22}$  has the same asymptotic form, i.e., the non-isothermal correction may not be small. However, estimates using the experimental values of  $\kappa_{22}$  and the values of  $\kappa_{21}$  and  $\kappa_{23}$  calculated from measurements of the thermomagnetic quantities show that the corrections for non-isothermy to the measured components of the tensor  $\hat{\alpha}$ , both diagonal and off-diagonal, did not exceed 5% in the most unfavorable case ( $\mathbf{H} \parallel \mathbf{C}_2$ ,  $T = 4^\circ \text{K}$ ), and were 1% and less in all the remaining cases. We could therefore assume that the experimentally determined quantities under isothermal in the entire temperature region under consideration, and compare them directly with the theory.

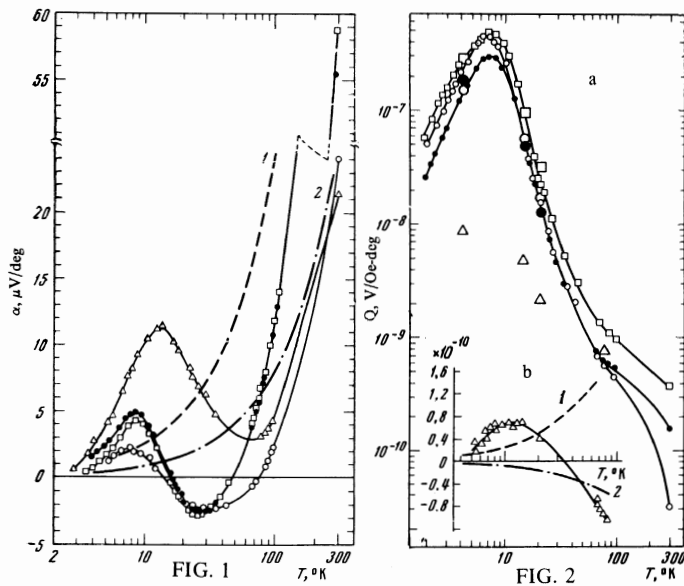
Figures 1 and 2 show the temperature dependence of the thermoelectric power (without a magnetic field) and of the Nernst coefficient (measured in a magnetic field of  $22 \text{ kOe}$ ) for the specimens Sb I, Sb II, and Sb III, and for an antimony specimen doped with tin up to a hole density  $p = 2.5 \times 10^{20} \text{ cm}^{-3}$  (henceforth designated Sb IV), while Figs. 3-5 show the thermoelectric power and the Nernst coefficient for the same samples (at a different orientation of the magnetic field) as functions of the magnetic field at temperatures  $\sim 20$  and  $4^\circ \text{K}$ .

Attention is called to the nonmonotonic behavior (the presence of a maximum and a minimum) of the thermoelectric power in Fig. 1 (for all three pure specimens), the sign becoming negative in the temperature region  $20-70^\circ \text{K}$ .

Such a behavior can be due to the influence of dragging of holes by phonons (near  $8^\circ \text{K}$ ) and of electrons by phonons (near  $25^\circ \text{K}$ ), but the absolute value of the thermoelectric power is small and in the entire temperature interval it does not exceed the value obtained from estimates with allowance for the diffusion contribution only.

The temperature dependence of the thermoelectric power of antimony (without a magnetic field) in the temperature region  $77-700^\circ \text{K}$  was investigated earlier by Saunders and Oktu<sup>[2]</sup> and was satisfactorily interpreted with allowance for only the diffusion component for the acoustic scattering of electrons and holes.

The diffusion thermoelectric power calculated by us



in the temperature interval 2–100° K with allowance for only acoustic scattering has a monotonic temperature dependence and does not reverse sign. The diffusion thermoelectric power was estimated from the formulas given in the Appendix.

Doping the antimony with tin led to a complete compensation of the electrons, so that the Sb IV specimen contained carriers of only one sign. This caused a noticeable increase of the maximum thermoelectric power in the region of the lowest temperature (Fig. 1, experimental data—triangles) and revealed clearly the influence of the dragging of holes by phonons (the dashed and dash-dot curves 1 and 2 in Fig. 1 give estimates of the diffusion thermoelectric power for Sb IV in the case of hole scattering by ionized impurities ( $r = 3/2$ ) and acoustic phonons ( $r = -1/3$ ), respectively.

The Nernst coefficient for the specimen Sb IV is much smaller (Fig. 2b) than for the pure specimens (Fig. 2a), owing to the reduced hole mobility in the doped specimen, and turns out to be close to the pure diffusion value of the Nernst coefficient (curves 1 and 2 in Fig. 2b).

Analogous phenomena were observed in doped bismuth by Korenblit, Kuznetsov, and Shalyt<sup>[11]</sup>.

The influence of the dragging effect becomes most strongly pronounced for thermomagnetic phenomena in strong magnetic fields. Thus, for example, the value of the Nernst coefficient  $Q_{12}$  below nitrogen temperature is larger by approximately one order of magnitude than the value calculated with only the diffusion contribution taken into account (the corresponding data on Fig. 2a are represented by triangles; the parameter of the scattering mechanism was assumed to be the same for electrons and holes and to correspond to the acoustic one,  $r_+ = r_- = -1/2$ ). On the other hand, the diagonal components of the tensor of the magnetoelectric power in a magnetic field is so small when only the diffusion contribution is considered, that the corresponding calculation data are not shown in Figs. 3–5, since they could not be noted in the linear scale used in these figures (the calculated  $\alpha_{22}$  and  $\alpha_{33}$  amount only to 2–3 2–3  $\mu$  V/deg in a field  $H = 30$  kOe).

FIG. 1. Temperature dependence of the components of the thermoelectric power tensor  $\alpha_{11}^0$  ( $\square$ ),  $\alpha_{22}^0$  ( $\bullet$ ),  $\alpha_{33}^0$  ( $\circ$ ), measured on pure antimony single crystals Sb II, Sb I, and Sb III, and temperature dependence of the thermoelectric power ( $\Delta$ ) measured on an antimony single crystal doped with tin, Sb IV. Curves 1 and 2—calculated values of the diffusion thermoelectric power for the sample Sb IV for carrier scattering by ionized impurities and phonons, respectively.

FIG. 2. a) Temperature dependence of the Nernst coefficients  $Q_{21}$  ( $\circ$ ),  $Q_{32}$  ( $\bullet$ ),  $Q_{13}$  ( $\square$ ) (in absolute value), measured respectively on pure antimony single crystals Sb II, Sb I, and Sb III in a constant magnetic field  $H = 22$  kOe. The large symbols ( $\circ$ ,  $\bullet$ ,  $\square$ ) represent the calculated values of the Nernst coefficients ( $H = 22$  kOe) with allowance for the dragging effect at temperatures 4.2, 14.5, and 20.4° K. Triangles—calculated values of the diffusion component of the Nernst coefficient  $Q_{12}$  ( $H = 22$  kOe) for the acoustical scattering mechanism. b) Temperature dependence of the Nernst coefficient measured on a single crystal of antimony doped with tin, Sb IV, in a constant magnetic field  $H = 22$  kOe. Points—experiment. Curves 1 and 2—calculated values of the diffusion component of the Nernst coefficient for scattering by ionized impurities ( $r = 3/2$ ) and acoustic phonons ( $r = -1/2$ ), respectively.

Thus, below hydrogen temperature ( $T = 20.4^\circ$  K), the predominant contribution to the thermomagnetic phenomena is made by the dragging of the carriers by phonons.

The influence of the carrier dragging by phonons at low temperatures was already noted earlier<sup>[3–5]</sup>.

Near liquid-nitrogen temperature, the data on the dependence of the thermoelectric power and of the Nernst coefficient on the magnetic field do not contradict the assumption that there is no dragging effect, but there is no quantitative agreement between calculation and theory if only the diffusion component is taken into account (assuming purely acoustic scattering of the electrons and holes). In particular, calculations with  $r_+ = r_- = -1/2$  for  $\alpha_{22}$  and  $\alpha_{33}$  at  $H \parallel C_2$  underestimate the value of the Umkehr effect. Measurements of the Lorentz number and galvanomagnetic data<sup>[12,6]</sup> show that in the nitrogen region of temperatures the predominant scattering mechanism is probably intervalley scattering of electrons and holes. Our preliminary calculations of the thermomagnetic effect with allowance for intervalley scattering only shows that by selecting the constants of the interaction between the “intervalley” phonons and the electrons or holes it is possible to obtain satisfactory agreement between theory and experiment. The results of the measurements of the thermomagnetic phenomena at nitrogen temperatures will be discussed in greater detail in a separate article.

Let us examine the behavior of the thermomagnetic coefficients in the region of the dragging effect.

It is seen from Fig. 3 that at  $T = 20^\circ$  K one observes a linear dependence of  $\alpha_{22}$  and  $\alpha_{33}$  on the magnetic field if the latter is directed along  $C_2$ ,  $\alpha_{22}$  saturates if  $H \parallel C_3$  (curve 2 of Fig. 4).  $\alpha_{33}$  saturates at  $H \parallel C_1$ , while  $\alpha_{11}$  ( $H \parallel C_1$ ) and  $\alpha_{11}$  ( $H \parallel C_3$ ) exhibit a tendency to saturation (these data are not shown in the figures). Thus, we obtain asymptotic relations typical of the components of the tensor  $\hat{\alpha}$  in strong magnetic fields and predicted by the theory for the phonon contribution to the thermoelectric power (at  $n = p$ ).

The Nernst coefficient at hydrogen temperatures does not depend on the magnetic field (Figs. 3 and 4), likewise in agreement with the predictions of the theory (the case of strong magnetic field is satisfied at 20.4° K, starting with magnetic fields near 10 kOe<sup>[6]</sup>).

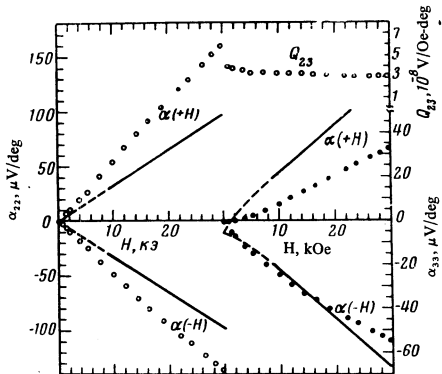


FIG. 3. Thermoelectric powers  $\alpha_{22}$  and  $\alpha_{23}$  and the Nernst coefficient  $Q_{23}$  vs. the magnetic field at  $\mathbf{H} \parallel \mathbf{C}_2$  and  $T \approx 20^\circ\text{K}$ . Points—experiment. Solid lines—calculated values with allowance for the dragging effect ( $n = p$ ).

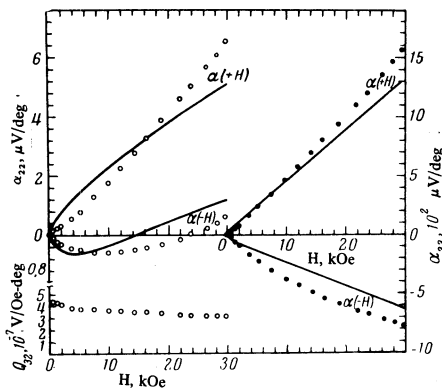
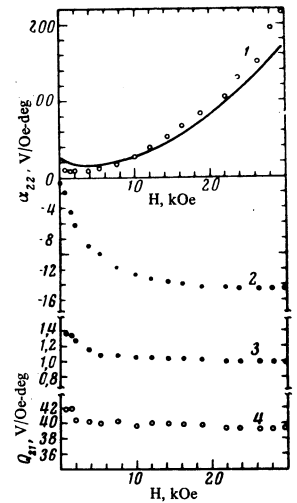


FIG. 5. Dependence of the thermoelectric powers  $\alpha_{22}$  and  $\alpha_{33}$  and of the Nernst coefficient  $Q_{23}$  on the magnetic field at  $\mathbf{H} \parallel \mathbf{C}_2$ ,  $T \approx 4^\circ\text{K}$ . Points—experiment, solid lines—calculated values with allowance for the dragging effect and the inequality of the electron and hole densities ( $\Delta N = p - n$ ).

In the helium temperature region, the dependences of the thermoelectric power tensor components on the magnetic field are greatly changed. Thus, at  $T = 4^\circ\text{K}$ , the component  $\alpha_{22}(\mathbf{H} \parallel \mathbf{C}_3)$  saturates already in a field close to 5 kOe (Curve 1 of Fig. 4), and then begins to increase more rapidly than linearly with increasing magnetic field. For  $\alpha_{22}$  and  $\alpha_{33}$  at  $\mathbf{H} \parallel \mathbf{C}_2$  in strong fields, the main contribution should be made by the term linear in  $H$ , which is responsible for the Umkehr effect, but it is apparently predominant only in fields up to 4 kOe, and in stronger fields there appears a considerable contribution that is even in the magnetic field, which leads even to a reversal of the sign of  $\alpha(-H)$  for  $\alpha_{22}(\mathbf{H} \parallel \mathbf{C}_2)$ , i.e., it begins to prevail over the Umkehr effect (Fig. 5). The variation Nernst coefficient is weaker, but in many cases it exhibits, in lieu of saturation, a weak decrease with the magnetic field (Fig. 5).

Such a behavior of the thermomagnetic coefficients at helium temperatures can be easily explained by taking into account the presence of a small density difference  $\Delta N = p - n$  in the investigated antimony specimens (it equals  $5 \times 10^{-4}N$  for Sb I,  $3 \times 10^{-4}N$  for Sb II, and  $1 \times 10^{-3}N$  for Sb III<sup>[6]</sup>). In this case the asymptotic behavior of the thermomagnetic coefficients, which is characteristic of the region of strong magnetic field

FIG. 4. Dependence of the thermoelectric power  $\alpha_{22}$  and of the Nernst coefficient  $Q_{21}$  on the magnetic field at  $\mathbf{H} \parallel \mathbf{C}_3$ . Curves 1 and 4 are for  $T \approx 4^\circ\text{K}$  and curves 2 and 3 for  $T \approx 20^\circ\text{K}$ . Points—experiment. Solid curve 1—calculated values of the thermoelectric power with allowance for the dragging effect and for the unequal electron and hole densities ( $\Delta N = p - n$ ).



(and for  $n = p$ ) ( $\alpha_{22} \sim H$ ,  $\alpha_{23} \sim H$ ,  $\alpha_{33} \sim H$  at  $\mathbf{H} \parallel \mathbf{C}_3$ ), is replaced by relations typical of the region of "intermediate" fields ( $n \neq p$ ) ( $\alpha_{22} \sim H^2$ ,  $\alpha_{23} \sim H^2$ ,  $\alpha_{33} \sim H^2$  at  $\mathbf{H} \parallel \mathbf{C}_2$ ;  $\alpha_{12} \sim H$ ,  $\alpha_{22} \sim H^2$  at  $\mathbf{H} \parallel \mathbf{C}_3$ ).

Estimates obtained with the aid of the values of  $\Delta N$  and the mobilities determined by us in<sup>[6]</sup> show that in accordance with the criteria (25) and (13) the transition region of the "intermediate" fields should set in at  $H \approx 12.5$  kOe for  $\mathbf{H} \parallel \mathbf{C}_3$  and  $H \approx 15$  kOe for  $\mathbf{H} \parallel \mathbf{C}_2$ . The case of "extremely strong" magnetic field was not realized in the employed magnetic fields (up to 30 kOe), owing to the very small density differences  $\Delta N$  (estimates of the field in which a transition to extremely strong fields should take place yield  $H \approx 800$  kOe).

At hydrogen temperatures, owing to the lower values of the mobility than in the helium region, one cannot expect an influence of  $\Delta N$  to appear up to fields on the order of 140 kOe (this agrees with the behavior of the galvanomagnetic coefficients at hydrogen temperatures<sup>[6]</sup>).

Consequently, the qualitative behavior of the thermomagnetic coefficients as a function of the magnetic field at hydrogen and helium temperatures is described very satisfactorily by a theory that takes electron and hole dragging by phonons into account.

We deemed it of interest to determine the partial thermoelectric powers of the electrons and holes and to compare the experimental values with the theoretical estimates.

The experimental values of the partial thermoelectric powers were determined by fitting with the aid of a computer. The components of the thermoelectric power tensor in a magnetic field were calculated using the formulas of Sec. 1 for the tensor  $\hat{\beta}$  and the formulas of<sup>[6]</sup> for the electric-conductivity tensor  $\hat{\sigma}$ , while the thermoelectric power tensor was determined from the relation  $\hat{\alpha} = \hat{\sigma}^{-1}\hat{\beta}$ . We used in the calculations the electron and hole mobilities determined in<sup>[6]</sup>, and at helium temperatures we took into account the inequality of the electron and hole densities,  $\Delta N = p - n$ . We used also the simplifying assumption that the mass ellipsoids of the holes and electrons can be replaced by ellipsoids of revolution, i.e.,  $\alpha_1 = \alpha_3$ , and that the tensors of the partial thermoelectric powers of the electrons and holes are diagonal in terms of the ellipsoid axes.

Partial thermoelectric powers of the electrons and holes in antimony at different temperatures in the region of phonon dragging (in  $\mu\text{V/deg}$ )

$\alpha_i^\pm$	T, °K			Theory ( $T_0 < T < T_f$ )
	4.2	14.5	20.4	
$\alpha_1^- = \alpha_3^-$	-15	-50	-50	-70 (0.812 k/e)
$\alpha_2^-$	-30	-160	-160	-1035 (12 k/e)
$\alpha_1^+ = \alpha_3^+$	30	8	8	55 (0.636 k/e)
$\alpha_2^+$	80	40	40	1635 (12 k/e)

The experimental partial thermoelectric powers of the electrons and holes (in terms of the ellipsoid axes), determined in this manner, are listed in the table for different temperatures.

The dependence of the thermoelectric power tensor components on the magnetic field for different magnetic-field orientations, calculated with these values of the partial thermoelectric powers, is shown by the solid curves in Figs. 3–5; the large circles in Fig. 2 show the Nernst coefficients calculated from the partial thermoelectric powers. For thermoelectric power without a magnetic field the agreement obtained is worse than for the thermomagnetic coefficients, since its absolute value is very small, and it is determined as a difference of two large quantities.

A theoretical estimate of the partial thermoelectric powers of the holes and electrons can be obtained from Korenblit's formulas<sup>[10]</sup>, in which the ellipsoidal shape of the equal-energy surfaces is taken into account. We used a somewhat cruder approximation, since we have assumed the phonon spectrum to be isotropic, and the ellipsoids to be strongly prolate

$$\beta = (m_2 - \bar{m}) / \bar{m} \gg 1, \quad \bar{m} = (m_1 m_3)^{1/2}, \quad (28)$$

$$\alpha_1 = \alpha_3 = 3\pi k / \beta e, \quad \alpha_2 = 12k / e$$

(the charge must be taken negative for electrons and positive for holes).

The partial thermoelectric powers of the holes and electrons in antimony, calculated in this manner, are listed in the last column of the table; they are the maximum possible values that should be realized for the case  $T_0 < T < T_f$  (and correspond to the value  $4k/3e$  in the case of an isotropic carrier spectrum).

Let us estimate  $T_0$  for the carriers in antimony. At first glance it is necessary to introduce two values of  $T_0$  for the mass ellipsoid:

$$T_{0\parallel} \approx 2\sqrt{2m_{\parallel}S^2\zeta^2} / k, \quad T_{0\perp} \approx 2\sqrt{2m_{\perp}S^2\zeta^2} / k,$$

which characterize the upper limit of the number of phonons that interact with carriers whose momentum is directed along or across the ellipsoid axis. Actually, however, a more correct estimate of the temperature  $T_0$  should be obtained not from the upper limits in the interval (3), but by comparing the first and second terms in the expansion of the exponential in the integrand in powers of  $\hbar\omega/kT$  (a value of  $T_0$  estimated in this manner indeed characterizes the transition from the region where the partial thermoelectric power does not depend on the temperature into the region where  $\alpha_k l$  decreases with temperature). Such an estimate yields

$$T_{0\parallel} \approx \frac{1}{k} \left( \frac{2}{15} m_{\parallel} S^2 \zeta^2 \right)^{1/2}, \quad T_{0\perp} \approx \frac{1}{k} \left( \frac{8}{15\pi} m_{\perp} S^2 \zeta^2 \right)^{1/2},$$

i.e., values much less than obtained with estimates based on the upper limit of the phase region of the phonons; in addition, there is practically no anisotropy of  $T_0$  (since the anisotropy is contained in almost the same manner in the first and second terms of the expansion in powers of  $\hbar\omega/kT$ ). For the holes and electrons in antimony we then obtain  $T_{0\perp} \approx 7.3^\circ\text{K}$  and  $T_{0\parallel} \approx 8.4^\circ\text{K}$  (estimates based on the upper limit would yield

$$T_{0\parallel}^{(+)} = 56^\circ\text{K}, \quad T_{0\perp}^{(+)} = 14^\circ\text{K}, \quad T_{0\parallel}^{(-)} = 65^\circ\text{K}, \quad T_{0\perp}^{(-)} = 18^\circ\text{K}.$$

Thus, at  $T_f > T_0$  one should expect the partial thermoelectric powers of both the electrons and the holes to be close to the values calculated from (28), at least near hydrogen temperatures. It is seen from the table, however, that the experimental partial thermoelectric powers are much lower than the calculated ones for both types of carrier; consequently, the case  $T_f < T_0$  is realized in antimony, and at hydrogen temperatures the phonon-phonon scattering prevails over phonon-electron scattering. This conclusion agrees with the results of<sup>[4]</sup>, where an analysis of the measured lattice thermal conductivity in antimony has shown that at a temperature on the order of  $30^\circ\text{K}$  the probability of the phonon-phonon scattering as a result of the Umklapp processes becomes comparable with the probability of phonon scattering by the carriers.

In all probability, the hydrogen temperature region for electrons is close to  $T_f$ , since a decrease of the temperature to  $4^\circ\text{K}$  leads to a decrease of the partial thermoelectric powers of the electrons, whereas for holes the partial thermoelectric powers increase with decreasing temperature.

Blewer, Zebouni, and Grenier<sup>[4]</sup> have shown that in the isotropic model it is possible to connect in a rather simple manner the contributions of the phonons to the thermoelectric tensor  $\hat{\beta}$  in strong magnetic fields with the phonon specific heat  $C_g$

$$\frac{\beta_{12}}{T} = -\frac{c}{TH} \left( C_{el} + \frac{1}{3} r C_g \right) = -\frac{\pi^2 k^2 c}{3H} \left[ D_{el} + r \frac{12\pi^2}{5} \frac{N}{k\Theta} \left( \frac{T}{\Theta} \right)^2 \right]$$

Where  $C_{el}$  and  $C_g$  are respectively the electron and phonon specific heats,  $\Theta$  is the Debye temperature, and  $D_{el}$  is the density of the electron states.

The experimental data<sup>[4]</sup> show that the "dragging force" coefficient  $r$  turns out to be close to unity, i.e., the dragging is complete. (All the excited phonons are predominantly scattered by the carriers,  $\nu(\mu) \approx \nu(\mu, S)$ ). (The isotropic model can serve as a reasonable approximation for the case when the magnetic field is oriented along the most symmetrical direction, i.e., parallel to  $C_3$ .)

If we use our data to plot  $\beta_{12}/T$  against  $T^2$ , then the slope, which describes the term  $rC_g/2$ , turns out to be close to the data of Blewer et al., i.e., the term  $rC_g$  is close in our case to the value of the phonon specific heat, and consequently the coefficient  $r$  is close to unity.

Thus, our results agree with the data of<sup>[4]</sup> and allow us to assume that the dragging is "complete" at helium temperatures, whereas at hydrogen temperatures it is weakened by the competition between the phonon-phonon processes and the phonon-carrier scattering.

Somewhat unexpected is the behavior of the partial thermoelectric powers of the holes, which increase on going from hydrogen to helium temperatures. If it is

assumed, however, that for holes the characteristic temperature  $T_f$  lies near helium temperatures, then this behavior becomes understandable. Such a situation can be realized if the hole-phonon interaction is weaker than the phonon-electron interaction, as is indicated also by the much higher mobility of the holes than that of the electrons, in spite of the rather small difference between their effective masses<sup>[6]</sup>.

In conclusion, the authors thank S. S. Shalyt for taking the initiative in this research and for useful advice, I. Ya. Korenblit for valuable remarks and a fruitful discussion of the results, and Yu. L. Sal'nikov for help in compiling the computer program.

#### APPENDIX

We present expressions for the diffusion contribution to the thermoelectric tensor  $\hat{\beta}$  for the cases when the magnetic field  $\mathbf{H}$  is oriented along the principal crystallographic axes. To calculate the tensor  $\hat{\beta}$ , besides the assumptions made concerning the model of the energy spectrum and the form of the relaxation time, considered in the first section of the article, it is assumed in addition that the relaxation time is described by a universal function of the carrier density  $\tau_{ij} = \tau_{ij}^0 \epsilon^{\mathbf{r}}$ , and the entire anisotropy is contained in the factors  $\tau_{ij}^0$  that do not depend on the energy. This form of the relaxation time was proved in<sup>[13,14]</sup> for bismuth telluride and bismuth, which belong to the same crystalline class  $D_{3d}^5$ .

In the case  $\mathbf{H} \parallel C_2 \parallel 1$ :

$$\beta_{11} = \frac{e}{T} \frac{N}{3} \frac{\pi^2}{3} (kT)^2 \sum_{\zeta_i} \frac{Z_i}{\zeta_i} \{ (r_i + 3/2) \mu_{i1} + (1 + \mathcal{E}_i(H/c)^2)^{-2} [I_i(r_i + 3/2) - (r_i - 3/2) I_i \mathcal{E}_i(H/c)^2 + 2(3r_i + 3/2) \mu_{i1} \mathcal{H}_i(H/c)^2 + 2(r_i + 3/2) \mu_{i1} \mathcal{H}_i \mathcal{E}_i(H/c)^4] \}, \quad (\text{A.1})$$

the quantities  $I_i$ ,  $\mathcal{H}_i$ , and  $\mathcal{E}_i$  were defined earlier,  $\zeta_i$  is the partial chemical potential of the holes or electrons:

$$\beta_{22} = \frac{e}{T} \frac{N}{3} \frac{\pi^2}{3} (kT)^2 \sum_{\zeta_i} \frac{Z_i}{\zeta_i} \{ (1 + \mathcal{H}_i(H/c)^2)^{-2} \times [(r_i + 3/2) \mu_{21} - (r_i - 3/2) \mu_{21} \mathcal{H}_i(H/c)^2] + (1 + \mathcal{E}_i(H/c)^2)^{-2} [(r_i + 3/2) \mathcal{E}_i - (r_i - 3/2) \mathcal{E}_i \mathcal{E}_i(H/c)^2] \}, \quad (\text{A.2})$$

$$\beta_{33} = \frac{e}{T} \frac{N}{3} \frac{\pi^2}{3} (kT)^2 \sum_{\zeta_i} \frac{1}{\zeta_i} \left\{ \left( 1 + \mathcal{H}_i \left( \frac{H}{c} \right)^2 \right)^{-2} \times [(r_i + 3/2) \mu_{31} - (r_i - 3/2) \mu_{31} \mathcal{H}_i(H/c)^2 + Z_i(2r_i + 3/2) \mathcal{H}_i(H/c) + Z_i \cdot 3/2 \mathcal{H}_i^2(H/c)^2 - (1 + \mathcal{E}_i(H/c)^2)^{-2} [(r_i + 3/2) \mu_{31} - (r_i - 3/2) \mu_{31} \times \mathcal{E}_i(H/c)^2 - Z_i \cdot 2(2r_i + 3/2) \mathcal{E}_i(H/c) - 3Z_i \mathcal{E}_i^2(H/c)^2] \right\}, \quad (\text{A.3})$$

$$\beta_{33} = \frac{e}{T} \frac{N}{3} \frac{\pi^2}{3} (kT)^2 \sum_{\zeta_i} \frac{Z_i}{\zeta_i} \left\{ \left( 1 + \mathcal{H}_i \left( \frac{H}{c} \right)^2 \right)^{-2} \times [(r_i + 3/2) \mu_{31} - (r_i - 3/2) \mu_{31} \mathcal{H}_i(H/c)^2] + (1 + \mathcal{E}_i(H/c)^2)^{-2} \times [2(r_i + 3/2) \mu_{31} - 2(r_i - 3/2) \mu_{31} \mathcal{E}_i(H/c)^2] \right\}; \quad (\text{A.4})$$

$$\beta_{12} = \beta_{13} = \beta_{21} = \beta_{31} = 0.$$

The asymptotic behavior of the components of the tensor  $\hat{\alpha}$  in the region of strong, "intermediate," and extremely strong fields is the same as for the phonon part of the tensor  $\hat{\alpha}$ .

For the case  $\mathbf{H} \parallel C_1 \parallel 2$ , we present only the asymptotic values for the tensor for the region of the "intermediate" fields, when they do not coincide with the asymptotic values of the phonon contribution to  $\hat{\alpha}$  (in strong and extremely strong fields they are the same for the diffusion and the phonon thermoelectric powers):

$$\begin{aligned} \alpha_{11} &\sim H^2, & \alpha_{12} &\sim H, & \alpha_{13} &\sim H, & \alpha_{21} &\sim H, \\ \alpha_{22} &\sim H^2, & \alpha_{23} &\sim H^0, & \alpha_{31} &\sim H, & \alpha_{32} &\sim H^2, \\ & & \alpha_{33} &\sim H^2. \end{aligned} \quad (\text{A.5})$$

In the case  $\mathbf{H} \parallel C_3 \parallel 3$

$$\beta_{11} = \beta_{22} = \frac{e}{T} N \frac{\pi^2}{3} (kT)^2 \sum_{\zeta_i} \frac{Z_i}{\zeta_i} \left( 1 + \mu_{i1} \mu_{21} \left( \frac{H}{c} \right)^2 \right)^{-2} \times [(r_i + 3/2)^{1/2} (\mu_{i1} + \mu_{21}) - (r_i - 3/2)^{1/2} (\mu_{i1} + \mu_{21}) \mu_{i1} \mu_{21} (H/c)^2], \quad (\text{A.6})$$

$$\beta_{12} = -\beta_{21} = \frac{e}{T} N \frac{\pi^2}{3} (kT)^2 \sum_{\zeta_i} \frac{1}{\zeta_i} \left( 1 + \mu_{i1} \mu_{21} \left( \frac{H}{c} \right)^2 \right)^{-2} \cdot [(2r_i + 3/2) \mu_{i1} \mu_{21} (H/c) + 3/2 \mu_{i1}^2 \mu_{21}^2 (H/c)^2], \quad (\text{A.7})$$

$$\beta_{33} = \frac{e}{T} N \frac{\pi^2}{3} (kT)^2 \sum_{\zeta_i} \frac{Z_i}{\zeta_i} \left\{ (r_i + 3/2) \mu_{31} - \left( 1 + \mu_{i1} \mu_{21} \left( \frac{H}{c} \right)^2 \right)^{-2} [(3r_i + 3/2) \mu_{i1} \mu_{21}^2 (H/c)^2 + (r_i + 3/2) \mu_{i1}^2 \mu_{21}^2 (H/c)^4] \right\}. \quad (\text{A.8})$$

The remaining coefficients are equal to zero.

It is interesting to note that in strong magnetic fields (in the sense of the criterion (23)) we have

$$\beta_{12} = \frac{\pi^2 k^2 T}{3} \left( \frac{H}{c} \right)^{-1} (D_+ + D_-), \quad (\text{A.9})$$

where  $D_{\pm} = 3N/2\zeta_{\pm}$  is the effective density of states of the holes and electrons. Grenier and co-workers<sup>[3,4]</sup> used this formula to determine the total density of states of the carriers from measurements of the Nernst coefficient in a strong magnetic field, and obtained a result that agrees well with the data that follow from the measurements of the specific heat.

The asymptotic values of  $\hat{\alpha}$ , just as in the case  $\mathbf{H} \parallel C_2$ , coincide in all regions of the magnetic fields with the asymptotic behavior of the phonon thermoelectric power.

<sup>1</sup>L. M. Falicov and P. J. Lin, Phys. Rev. **141**, 562 (1966); J. Ketterson, O. Beckman, and G. Hornfeldt, J. Phys. Chem. Solids **25**, 1339 (1964); L. R. Windmiller and M. G. Priestly, Solid State Commun. **3**, 199 (1965); W. R. Datars and J. Vanderkooy, IBM J. Res. Dev. **8**, 247 (1964); N. B. Brandt, N. Ya. Minina, and Chou Chen-ch'ang, Zh. Eksp. Teor. Fiz. **51**, 108 (1966) [Sov. Phys.-JETP **24**, 73 (1967)]; L. R. Windmiller, Phys. Rev. **149**, 472 (1966).

<sup>2</sup>G. A. Saunders and Ö. Öktü, J. Phys. Chem. Solids **29**, 327 (1968)

<sup>3</sup>C. G. Grenier, J. R. Long, J. M. Reynolds, and N. H. Zebouni, Proc. 9th Int. Conf. Low. Temp. Physics, Part B, Plenum Press, Ohio, 1965, p. 302; J. R. Long, C. G. Grenier, and J. M. Reynolds, Phys. Rev. A **140**, 187 (1965).

<sup>4</sup>R. S. Blewer, N. H. Zebouni, and C. G. Grenier, Phys. Rev. **174**, 700 (1968).

<sup>5</sup>N. A. Red'ko and S. S. Shalyt, Fiz. Tverd. Tela **10**, 1557 (1968) [Sov. Phys.-Solid State **10**, 1233 (1968)].

<sup>6</sup>M. S. Bresler and N. A. Red'ko, Zh. Eksp. Teor. Fiz. **61**, 287 (1971) [Sov. Phys.-JETP **34**, 149 (1972)].

<sup>7</sup>A. L. Natadze and A. L. Éfros, Fiz. Tverd. Tela **4**, 2931 (1962) [Sov. Phys.-Solid State **4**, 2149 (1963)].

<sup>8</sup>L. E. Gurevich and I. Ya. Korenblit, Fiz. Tverd. Tela **6**, 856 (1964) [Sov. Phys.-Solid State **6**, 661 (1964)].

<sup>9</sup>L. É. Gurevich and I. Ya. Korenblit, Fiz. Tverd. Tela **9**, 1195 (1967) [Sov. Phys.-Solid State **9**, 932 (1967)].

<sup>10</sup>I. Ya. Korenblit, Fiz. Tekh. Poluprovodn. **2**, 1425 (1968) [Sov. Phys.-Semicond. **2**, 1192 (1969)].

<sup>11</sup>I. Ya. Korenblit, M. E. Kuznetsov, and S. S. Shalyt, Zh. Eksp. Teor. Fiz. **56**, 8 (1969) [Sov. Phys.-JETP **29**, 4 (1969)].

<sup>12</sup>N. A. Red'ko, M. S. Bresler, and S. S. Shalyt, Fiz. Tverd. Tela **11**, 3005 (1969) [Sov. Phys.-Solid State **11**, 2435 (1970)].

<sup>13</sup>I. Ya. Korenblit, Fiz. Tverd. Tela **2**, 3083 (1960) [Sov. Phys.-Solid State **2**, 2738 (1961)].

<sup>14</sup>A. G. Samoïlovich and I. I. Pinchuk, Fiz. Met. Metalloved. **20**, 663 (1965).